

Rapid radiative decay of charged excitons

D. Sanvitto,^{1,2} R. A. Hogg,¹ A. J. Shields,¹ D. M. Whittaker,¹ M. Y. Simmons,² D. A. Ritchie,² and M. Pepper^{1,2}

¹*Toshiba Research Europe Limited, Cambridge Research Laboratory, 260 Cambridge Science Park, Milton Road, Cambridge, CB4 0WE, United Kingdom*

²*Cavendish Laboratory, Madingley Road, Cambridge, CB3 0HE, United Kingdom*

(Received 1 September 2000)

We discuss the decay process of free trions, which differs radically from that of the neutral exciton or localized trions. A theoretical model for the decay time of free trions shows that due to the three particle decay process a rapid radiative decay, compared to the neutral exciton, is expected. We demonstrate the rapid decay of negatively charged excitons in remotely doped GaAs/AlGaAs quantum wells (QW's) experimentally and show the effects of temperature and well-width on the decay of free negatively charged excitons.

Many of the optical properties of semiconductors are dominated by excitonic effects. This semiconductor analog of the hydrogen atom has allowed many physical effects to be studied. Only a small fraction of excitons (those close to $\mathbf{k}=0$) in a thermalized population may decay into photons due to energy-momentum conservation in the recombination process.¹ Recently, charged excitons or trions, the semiconductor analog of H^- and H_2^+ , have been observed in doped semiconductor QW's (Refs. 2 and 3) and unintentionally doped QW's.⁴ This simple, controllable analog of a two electron atom can be expected to open up many avenues of research, for example concerned with the Coulomb and exchange interactions. We show here experimentally and theoretically that the three particle decay process of the charged exciton results in rapid radiative decay compared to neutral excitons, which cannot be accounted for by the difference in degeneracy of the two species of excitons. In essence, this is because the transfer of excess momentum to the electron left behind after trion recombination relaxes the condition that only $\mathbf{k}=0$ excitons can recombine. Since most semiconductors contain excess charge, even if not intentionally doped, due to the background impurity concentration, we suggest that this effect is important for recombination in all semiconductors.

Until now the study of trion decay dynamics have been concerned with localized negatively charged excitons, which may in essence be considered to be similar to localized neutral excitons.⁵ The only other study of free charged excitons indicated a decay time of the charged exciton four times more rapid than that of the neutral exciton.⁶ In that study the decay of neutral and charged exciton was considered to differ only in the spin degeneracy of the different species of excitons. In this work we discuss the fundamental differences in the decay process of a thermalized population of charged and neutral excitons.

The radiative recombination of an exciton (X) in a quantum well is governed by the conservation of energy and momentum (center-of-mass \mathbf{k} -vector) between the initial and final state. The lack of translational invariance normal to the plane of a quantum well relaxes the requirement for \mathbf{k} -vector conservation in that direction. Figure 1(a) shows schematically the dispersion of the exciton center of mass in the plane of the quantum well. Only excitons within the light cone,

defined by $E_{\text{photon}} = \hbar k$, satisfy \mathbf{k} -vector conservation and may recombine radiatively. Thus only excitons of energy $E \leq E_0 = \hbar^2 k^2 / 2M$ (typically for GaAs/AlGaAs QW $E_0 \sim 100 \mu\text{eV}$) can couple to photons. Excitons which lie outside the light-cone, are therefore nonradiative (so-called dark states). A consequence of the presence of the dark states is that the average decay time of a thermalized exciton population is typically $\sim \text{ns}$,¹ while the calculated intrinsic decay time of an exciton at $\mathbf{k}_{\parallel}=0$ is $\sim 25 \text{ ps}$.⁷

Figure 1(b) shows schematically the decay process of a negatively charged exciton (X^-), the bound state of two electrons and a hole. In this case charged excitons of large \mathbf{k} -vector may recombine, the mismatch in \mathbf{k} -vector between the charged exciton and the photon being given up to the electron. All charged exciton states are therefore radiative. The oscillator strength of the radiative transition is, however, a function of the momentum of the X^- with an exponential reduction with \mathbf{k}_{\parallel} .⁸

This is a simplified picture for both the neutral and charged exciton as exciton-phonon scattering, and exciton-exciton scattering can profoundly affect the radiative decay process by mixing states of different \mathbf{k} -vector together. These scattering effects broaden in energy the excitonic transition, giving it a homogeneous linewidth, Γ_h . As a consequence of

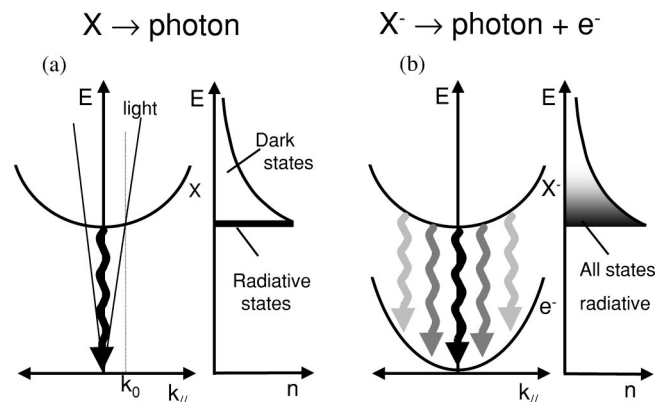


FIG. 1. Schematic diagram of dispersions, thermalized exciton distribution, and decay processes for (a) X and (b) X^- . Vertical axis corresponds to energy, while horizontal axes are total center-of-mass \mathbf{k} -vector and exciton number.

including these scattering events, excitons within a slightly larger radiative zone may recombine radiatively.⁹

The radiative decay time for QW excitons is calculated using Fermi's Golden rule. For the neutral exciton the final state corresponds to the crystal in its ground state and a photon with momentum $\mathbf{q}(\mathbf{k}_{//}, k_z)$ where $\mathbf{k}_{//}$ is the in-plane momentum and k_z is the momentum normal to the QW plane. The decay rate of the excitons as a function of $\mathbf{k}_{//}$ for each photon polarization is obtained. In order to include thermalization effects, the decay rate is averaged over a Boltzmann distribution of occupied exciton states.⁷ The oscillator strength of excitons in the light cone is shared between all states within Γ_h of E_0 .⁹ The decay time is averaged over the singlet ($J=0$) and optically forbidden triplet ($J=1$) states. For a temperature T such that $k_B T \gg E_0$ (where k_B is Boltzmann's constant), the final decay time of a thermalized exciton population, τ_X , as a function of temperature T is given as:

$$\tau_X = \frac{3}{2E_0} \tau_0 \left(k_B T + \frac{3}{5} E_0 \right) f(\Gamma_h^X, T), \quad (1)$$

where $f(\Gamma_h, T) = \hbar \Gamma_h / k_B (1 - e^{-\hbar \Gamma_h / k_B T}) k_B T$, and τ_0 is the calculated intrinsic radiative decay time of an exciton at $\mathbf{k}_{//} = 0$.⁷ This expression is derived combining the formalism used in Refs. 7 and 9, but using a second order expansion in terms of $E_0 / k_B T$.

To calculate the decay time for X^- we weight the Boltzmann distribution with the calculated optical matrix element. The decay time of the thermalized X^- population, τ_{X^-} , is given as:

$$\tau_{X^-} = \frac{3 \pi \hbar^2}{2 m_e \epsilon_1 E_0} \frac{|\psi_X(0)|^2}{\left| \int d^2 \rho \psi_{X^-}(0, \rho) \right|^2} \times \tau_0 \left(k_B T + \frac{m_e}{M_X} \epsilon_1 \right) f(\Gamma_h^{X^-}, T), \quad (2)$$

where \hbar is the Planck constant, m_e is the electron mass, ϵ_1 describes the exponential dependence of the spatial part of the optical matrix element ($M = M_0 e^{-\epsilon / \epsilon_1}$) on the X^- wave vector,¹⁰ $|\int d^2 \rho \psi_{X^-}(0, \rho)|^2$ and $|\psi_X(0)|^2$ are the overlap integrals for the radiative recombination of X^- and X , respectively. Equation (2) is expressed such that the decay of a thermalized population of X and X^- can be compared by taking into account the ratio between the integral of the spatial wavefunction parts and the exponential decay of X^- oscillator strength with $\mathbf{k}_{//}$.

High quality remotely doped GaAs/Al_{0.33}Ga_{0.67}As QW's have been grown by molecular beam epitaxy³ on GaAs substrates. We illustrate our arguments with spectra taken on a 300 Å or 100 Å GaAs QW, topped with 600 Å undoped Al_{0.33}Ga_{0.67}As and 2000 Å Si doped (10^{17} cm^{-3}) Al_{0.33}Ga_{0.67}As. The excess electron density is varied by applying a voltage between the Schottky NiCr gate evaporated on top surface of the sample and an Ohmic contact to the QW layer in order to allow the excess electron density in the QW to be controlled. This permits the study of neutral and negatively charged excitons in the same sample.

Time resolved photoluminescence (PL) was obtained using a mode locked Ti:Sapphire laser with repetition rate of

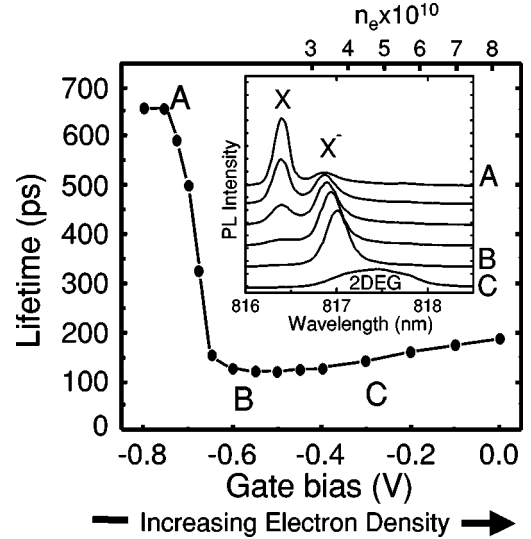


FIG. 2. Luminescence decay time for a 300 Å QW as a function of gate bias (and hence excess electron density). The inset shows PL spectra recorded at various biases where the luminescence is dominated by recombination of neutral (X) (A) and charged excitons (X^-) (B), and by recombination of excess electrons with minority holes (2DEG) (C). The top scale gives the excess carrier density (n_e) from a PL lineshape analysis.

82 MHz, pulse width of ~ 1 ps at a power density which creates $\sim 2 \times 10^{17} \text{ cm}^{-2}$ electron hole pairs within the quantum well with each pulse. The luminescence was dispersed by a spectrometer and detected by a streak camera operating in syncscan mode, with a temporal resolution of ~ 8 ps. The spectral width of the laser is sufficiently small to allow the resonant excitation of only one of the two exciton species. Resonant excitation was performed using linearly polarized excitation light and detecting the cross linearly polarized emission.

Figure 2 shows the decay time obtained by nonresonant time resolved PL on a 300 Å QW as a function of applied gate bias (and hence excess electron density). The additional scale shows how the excess electron density changes with applied front-gate bias by analysis of the PL lineshape. At biases below -0.45 V the excess electron density is not expected to be a linear function of front gate bias.¹¹ The inset plots PL spectra obtained at selected biases. At each bias, a single decay time is observed for X and X^- , showing the two exciton populations to be in thermodynamic equilibrium.⁶ Notice that the decay time decreases sharply with increasing gate bias. The fact that the decay time changes dramatically over this bias range, yet the integrated PL intensity remains constant, indicates that the decay is predominantly radiative and nonradiative processes can be ignored. For a gate bias of -0.75 V (point A), for which the electron density of the QW is minimized and the PL spectrum is dominated by X (see inset), a relatively long decay time of 660 ps is observed. The electron density increases with gate bias resulting in a transfer of PL intensity from X to X^- , reflecting the relative population of the two species. Notice in Fig. 2 that the transfer of PL intensity is accompanied by a sharp decrease in the decay time. The decay time reaches a minimum of 110 ps at point B where the exciton population is composed almost entirely of X^- . Thus, as ex-

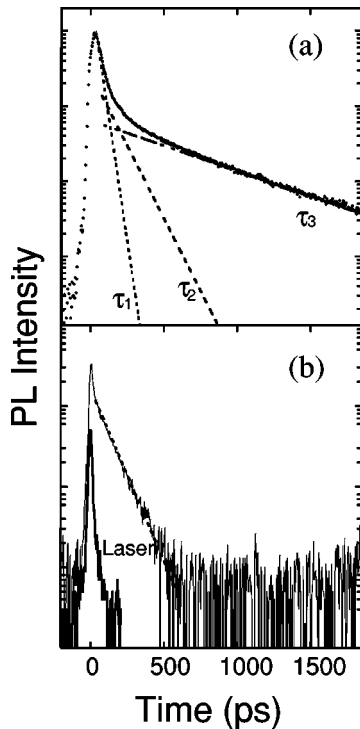


FIG. 3. X (a) and X^- (b) decay profiles obtained with the excitation pulse resonant with X and X^- transitions, respectively.

pected, we observe a faster decay when the exciton population comprises charged excitons, than when it is mostly neutral excitons. This is in contrast to the decay of bound excitons which exhibit a decay time longer than that of free excitons.¹² For the case where X dominates the PL spectra there is still a sizeable X^- population, as evidenced by the weak X^- peak in spectrum A, and the true X decay time is not measured. By comparing the measured decay time, the intensity ratio of the X and X^- peaks, and the decay time of X^- (when only X^- is present) the true decay time of the exciton can be determined.⁶ The X decay time is thus determined to be 930 ps. The X^- decay is therefore almost one order of magnitude faster than that of X, which cannot be explained by the increased degeneracy of the charged exciton alone.⁶

In order to access directly the radiative decay rate of excitons, it is necessary to use resonant photoexcitation,^{13,14} for which the excitation energy is equal to the exciton energy. The temporal decay of luminescence due to X after resonant excitation of X by a pulse at $t = 0$ is shown in Fig. 3(a). This data was obtained at a gate bias for which X dominates the luminescence spectra. A best fit to the data is obtained using three exponential terms with decay times of 30 ps, 140 ps, and 660 ps. On the other hand, a considerably worse fit is obtained by using only one or two exponential terms. We assign these three lifetimes to the decay of the coherently excited exciton population (resonant Rayleigh scattering) for the most rapid decay (30 ps), to the excitons dephased but not yet thermalized (140 ps), and to the thermalized exciton population for the longest decay time (660 ps). The slow decay, which is very close to that obtained by nonresonant excitation, indicates that the exciton population thermalizes to the same temperature (i.e., that of the lattice) regardless of the excitation conditions.

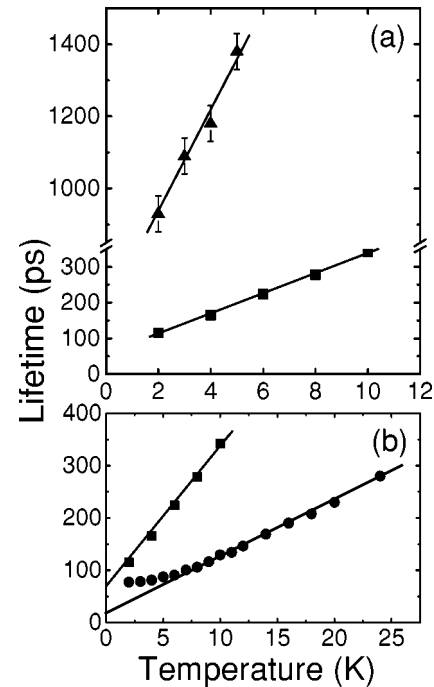


FIG. 4. Temperature dependence of decay time for (a) X (triangles) and X^- (squares) in a 300 Å QW, and (b) X^- in the 300 Å QW (squares) and 100 Å QW sample (circles). Lines are a linear fit to the data.

Figure 3(b) shows the temporal evolution of the X^- luminescence obtained under resonant excitation of X^- . This data was obtained at a bias where only X^- is observed in the luminescence spectra. In contrast to the case for resonant excitation of X, only a single exponential decay is observed. As the decay time is the same as that obtained with nonresonant excitation we attribute this decay to the thermalized X^- population. The dependence of this decay time with temperature, discussed later also indicates that the X^- is free. The spike at $t=0$ is symmetric and identical in form to the excitation laser. We therefore attribute it to light scattered from imperfections on the sample surface. It is intriguing to note that there is no resonant Rayleigh scattered light or cold X^- decay observed in Fig. 3(b). Two factors may be responsible for these effects. First, the interaction of a $\mathbf{k} \sim 0$ photon and a thermal bath electron results in the formation of an X^- of finite \mathbf{k}_\parallel , see Fig. 1(b). Second, due to the charge of X^- , which is expected to scatter efficiently with excess electrons, the X^- population may have a subpicoseconds thermalization time, much shorter than that for X. Conversely, X formation maintains its phase with the incident light, scattering coherently in random direction giving rise to a finite dephasing time (RRS). And then relaxes thermalizing to the lattice temperature forming a Boltzmann distribution in \mathbf{k}_\parallel space.

Figure 4(a) plots the temperature dependence of the decay time of X (adjusted for the presence of X^-)⁶ and X^- in a 300 Å QW obtained by resonant excitation. Linear dependencies of the decay times upon temperature for free X and X^- predicted by Eqs. (1) and (2) are observed. Figure 4(b) shows the temperature dependence of the X^- decay for the 300 Å and 100 Å QW samples. For the 100 Å QW sample X^- displays a rather temperature insensitive decay below 7 K, changing to a linear dependence for $T > 7$ K. We

interpret this as due to localization of X^- by interface roughness in the 100 Å QW at low temperature.⁵ Consistent with this the 100 Å QW sample exhibited a 1 meV Stoke shift between the X^- PL and PLE indicating a larger degree of localization compared to the 300 Å sample, which exhibited negligible Stokes shift.

From the equations (1) and (2) we see that the rate of change of the free X and free X^- decay time with temperature [Fig. 4(a)] provides a comparison of the overlap integrals for radiative recombination of X and X^- . In addition, for free X^- the rate of change of decay time with temperature, and the intercept at $T=0$, are also governed by the radiative recombination overlap integral. A comparison of the ratio of the gradients and intercepts in Fig. 4(b) allows the effect of QW width on the X^- radiative recombination overlap integral to be determined. In order to provide a theoretical estimate of these ratios we have obtained X and X^- wavefunctions by solving the Schrödinger equation for the relative motion using a basis of single particle states in a fictitious magnetic field, i.e.,

$$\psi_{X^-}^s = \sum_{\{lnm\}} \alpha_{\{lnm\}} \chi_{l_1}(z_{e_1}) \chi_{l_2}(z_{e_2}) \chi_{lh}(z_h) \times \frac{1}{\sqrt{2}} [\phi_{n_1 m_1}(\rho_a) \phi_{n_2 m_2}(\rho_b) + \phi_{n_1 m_1}(\rho_b) \phi_{n_2 m_2}(\rho_a)]. \quad (3)$$

And

$$\psi_{X^0} = \sum_{\{lnm\}} \alpha_{\{lnm\}} \chi_l(z_e) \chi_{lh}(z_h) \phi_{nm}(\rho). \quad (4)$$

Where the $\chi(z)$ are the electron and hole bound states in the quantum well, ϕ_{nm} is a symmetric gauge Landau level wave-

function and ρ_a, ρ_b are the in-plane separations of the hole from each of the electrons. The notation $\{lnm\}$ represents the quantum numbers $l_{e_1}, l_{e_2}, l_h, n_1, m_1, n_2, m_2$. The Landau level states form a convenient basis to calculate the bound states of the system allowing us to adapt the formalism of Ref. 15 to obtain accurate solutions to the X^- problem, though of course the absence of a magnetic field leads to additional kinetic matrix elements coupling the basis states. The inclusion of higher quantum well levels ($l > 1$) is particularly important for the 300 Å quantum well, where the effects of axial correlations are very significant. The calculations predict the ratio $(d\tau_X)/(dT)/(d\tau_{X^-}/dT)$ for the 300 Å QW sample to be 5.0. The experimental results give a ratio of 5.7, in good agreement with the predictions. The ratio of the gradients $(d\tau_{X^-}/dT)$ and intercepts (τ_{X^-} at $T = 0$) for the X^- decay in the 300 Å and 100 Å QW samples provide a comparison of the X^- oscillator strengths. Our model predicts the oscillator strength of X^- in the 100 Å QW to be ~ 2 times that of the 300 Å QW. The experimentally determined ratios are 2.6 and 2.7, again in good agreement.

In conclusion, we have discussed the fundamental difference in the decay processes of neutral and charged excitons, and have shown how the three particle charged exciton has a rapid radiative decay. Trions are only observed in high quality materials due to the requirement for spectroscopically resolving the trion and exciton that the second carrier binding energy is larger than the transition broadening. However, in the case where the exciton and trion lines cannot be resolved spectroscopically it seems likely that excess carriers will still strongly modify the recombination dynamics. This effect could also be important in nominally undoped structures, as typical background impurity concentrations are sufficient to produce a significant trion population.

¹J. Feldmann *et al.*, Phys. Rev. Lett. **59**, 2337 (1987).

²K. Kheng *et al.*, Phys. Rev. Lett. **71**, 1752 (1993).

³A. J. Shields *et al.*, Phys. Rev. B **51**, 18 049 (1995).

⁴J. L. Osborne *et al.*, Phys. Rev. B **53**, 13 002 (1996).

⁵G. Finkelstein *et al.*, Phys. Rev. B **58**, 12 637 (1998).

⁶A. Ron *et al.*, Solid State Commun. **97**, 741 (1996).

⁷L. C. Andreani, F. Tassone, and F. Bassani, Solid State Commun. **77**, 641 (1991).

⁸B. Stébé, E. Feddi, A. Ainane, and F. Dujardin, Phys. Rev. B **58**, 9926 (1998).

⁹D. S. Citrin, Phys. Rev. B **47**, 3832 (1993).

¹⁰A. Esser, E. Runge, R. Zimmermann, and W. Langbein, Phys. Stat. Solidi A **178**, 489 (2000).

¹¹R. Küchler, G. Abstreiter, G. Böhm, and G. Weimann, Semicond. Sci. Technol. **8**, 88 (1993).

¹²J. P. Bergman *et al.*, Phys. Rev. B **43**, 4765 (1991).

¹³B. Deveaud *et al.*, Phys. Rev. Lett. **67**, 2355 (1991).

¹⁴A. Vinattieri *et al.*, Phys. Rev. B **50**, 10 868 (1994).

¹⁵D. M. Whittaker and A. J. Shields, Phys. Rev. B **56**, 15 185 (1997).